fluctuations, short-wavelength modes have amplitudes that are suppressed because these modes oscillated as acoustic waves during the radiation epoch whereas the amplitude of long-wavelength modes grew during both radiation and matter epochs. The separation between short and long wavelengths corresponds to the Hubble distance at the moment of matter-radiation equality, $a(t_{\rm eq}) = a_0 1.68 \Omega_\gamma / \Omega_{\rm M}$ and to a present wavelength of $\lambda_{\rm eq} \sim 600\, h_{70}^{-1}{\rm Mpc} \times 0.27/(\Omega_{\rm M} h_{70})$.

The most important methods for measuring $\Omega_{\rm M}$ and Ω_Λ are "geometrical" methods that use type Ia supernovae as standard candles and the sound horizon at recombination as a standard ruler seen in the matter and CMB fluctuation spectra. These techniques are described in Chap. 5.

Finally, we note that $\Omega_{\rm M}$ can be deduced from the abundance of galaxy clusters and from the gravitational lensing galaxies by large-scale structure if one uses information of the mass fluctuation spectrum (Chap. 7).

Exercises

2.1 The luminosity of a typical galaxy is $\sim 2 h_{70}^{-2} \times 10^{10}\, L_\odot$ and the mean energy of stellar photons is $\sim 2\,{\rm eV}$. What is the photon flux (in ${\rm m^{-2}\,s^{-1}}$) of a galaxy of redshift z ($z \ll 1 \;\Rightarrow R \sim z d_H$)?

Compare the photon flux from the nearest large galaxies ($R \sim 1$ Mpc) with the photon flux from the nearest stars ($R \sim 1$ pc). (This calculation should explain why most objects visible to the naked eye are stars.)

2.2 The luminosity density of the universe is $\sim 1.2\ h_{70} 10^8 L_\odot\,{\rm Mpc^{-3}}$. Supposing that stellar light output has been relatively constant since the formation of the first stars about one Hubble time ago, estimate the number of photons ($E \sim 2$ eV) that have been produced by stars. Compare the number of stellar photons with the number of CMB photons. (This problem will be treated more rigorously in Exercise 5.12.)

Stellar energy is mostly produced by the fusion of hydrogen to helium $4{\rm p} \rightarrow {}^4{\rm He} + 2{\rm e}^+ + 2\nu_{\rm e}$. This transformation occurs through a series of reactions in stellar cores that liberate a total of ~ 25 MeV. After thermalization, the energy emerges from stellar surfaces in the form of starlight. Estimate the number of protons (per ${\rm Mpc}^3$) that have been transformed into helium over the last Hubble time. Compare this number with the number of protons available $n_{\rm b} \sim \Omega_{\rm b} \rho_{\rm c} / m_p$.

2.3 Estimate the contribution to the universal photon mean free path of the following processes:

- Thomson scattering of photons on free electrons of number density $n_{\rm e} \sim n_{\rm b}$.
- Absorption by stars of number density $n_{\rm stars} \sim \Omega_{\rm stars} \rho_{\rm c} / M_\odot$, $\Omega_{stars} \sim 0.0023$ and cross-section $\sim \pi R_\odot^2$.

- Absorption by dust in galaxies with $n_{\rm gal} \sim 0.005$ Mpc^{-3} and cross-section $\sim \epsilon \pi R_{\rm gal}^2$ where $R_{\rm gal} \sim 10$ kpc and the fraction of visible light absorbed when passing through a galaxy is $\epsilon \sim 0.1$.

Compare these distances with d_H ($\sim$ the distance of the most distant visible objects). Is the universe "transparent"? (Section 5.7 will treat this problem more rigorously.)

2.4 Supposing that we can only measure redshifts, angles, and photon fluxes, explain the factors of h_{70} in (2.9), (2.10), and (2.11) as well as the absence of such factors in (2.12).

2.5 By comparing the apparent magnitudes of LMC Cepheids (Fig. 2.5) to the apparent magnitudes of Cepheids in the galaxy NGC 1365 (Fig. 2.28), estimate the ratio of the NGC 1365 distance to the LMC distance. If the LMC distance is taken to be 50 ± 5 kpc, what is the distance to NGC 1365.

NGC 1365 is a member of the Fornax galaxy cluster. The recession velocity of this cluster is 1441 km s^{-1}. Estimate H_0.

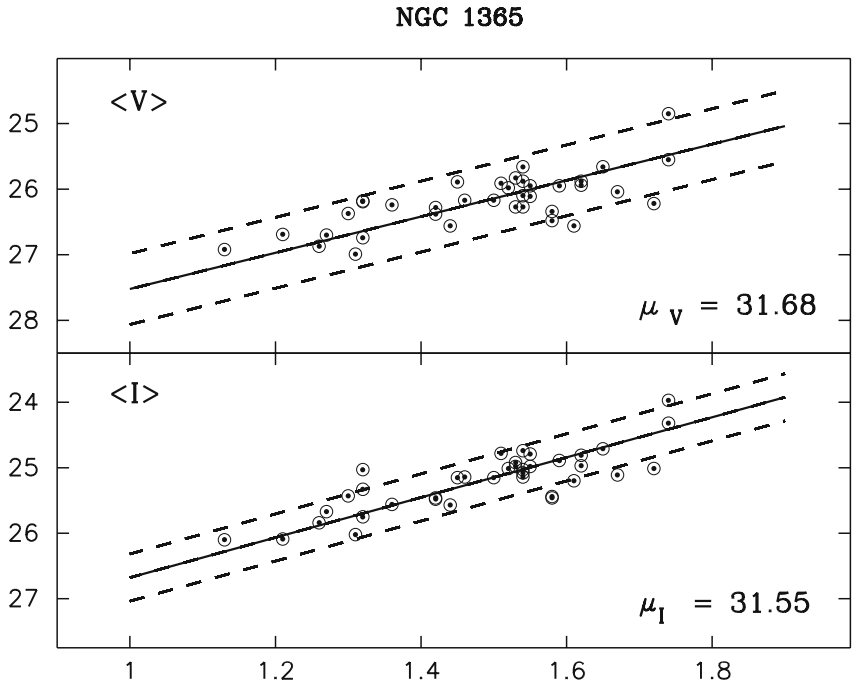

Fig. 2.28 The apparent magnitudes in the I and V bands of Cepheids in the galaxy NGC 1365 [53]. The magnitude is a linear function of log P where P is the Cepheid period in days

2.6 Abell-496 is a galaxy cluster whose properties were studied in [101].

(a) The recession velocity of A496 is 9885 km s^{-1}. What is its distance as a function of h_{70}?

(b) Figure 2.29 shows the angular distribution of the brightest galaxies in A496. Estimate the radius of the cluster.

(c) Figure 2.30 shows the distribution of recession velocities in the direction of A496. The accumulation near 9885 km s^{-1} corresponds to the cluster members. The width of this accumulation suggests that the line-of-sight velocity dispersion of A496 is $\Delta v \sim 715\,\mathrm{km\,s^{-1}}$. Use the virial theorem to estimate the cluster mass: ($GM/\Delta r \sim \Delta v^2$). A detailed study in [101] gives $M_{\mathrm{vir}} = (5.1 \pm 0.8) h_{70}^{-1} 10^{14} M_\odot$.

(d) The flux of visible light from A496 indicates a total luminosity of $L = 2.0\, h_{70}^{-2} \times 10^{12}\, L_\odot$. By assuming that M_{vir}/L is equal to the universal value ρ_{M}/J_0 with the universal luminosity density given by (2.10), estimate ρ_{M} and Ω_{M}.

(e) The X-ray spectrum indicates that the temperature of the intergalactic gas in A496 is 4 ± 1 keV. The X-ray flux allows one (Exercise 2.10) to estimate the total mass and the total mass of intergalactic gas. For A496, the total mass within $0.7\, h_{70}^{-1}$ Mpc of the cluster center is $(1.7 \pm 0.4) h_{70}^{-1} \times 10^{14} M_\odot$ and the total gas mass within the same radius is $(1.4 \pm 0.5) h_{70}^{-5/2} \times 10^{13} M_\odot$. Assuming that the ratio between baryonic mass and total mass of A496 is equal to the universal value, estimate $\Omega_{\mathrm{b}}/\Omega_{\mathrm{M}}$.

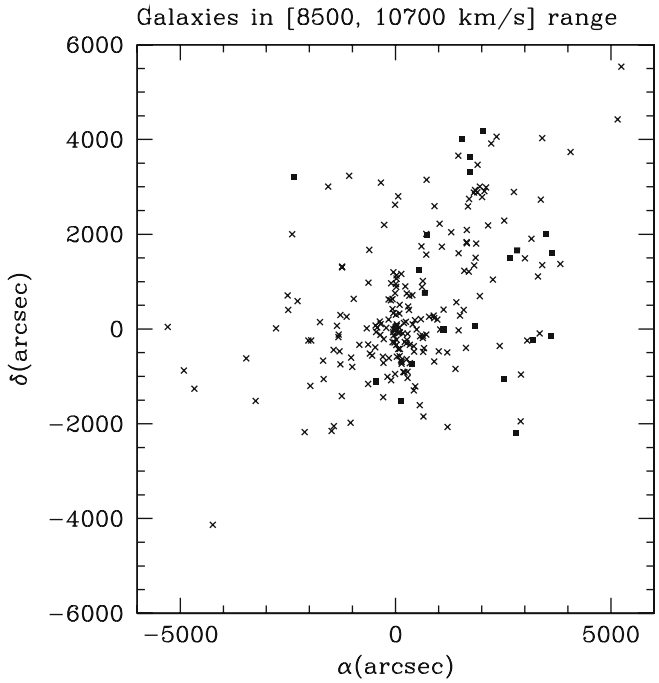

Fig. 2.29 The angular distribution of bright galaxies in A496 [101]

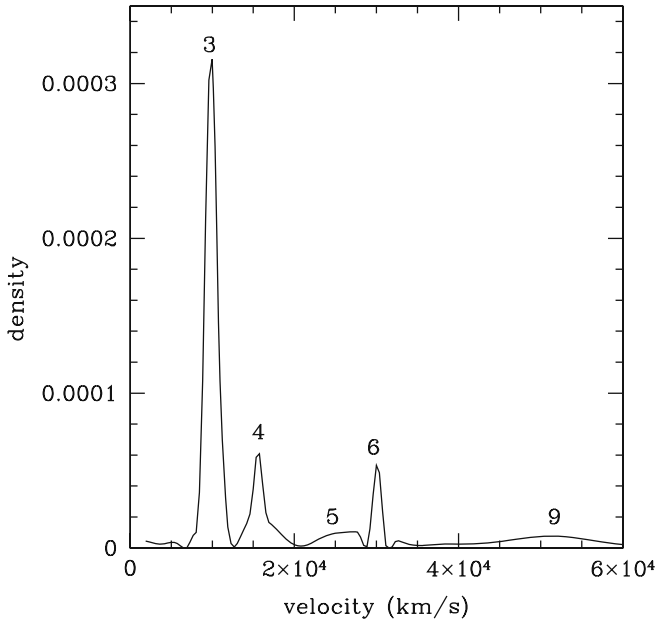

Fig. 2.30 The distribution of recession velocities in the direction of the A496 [101]. The accumulation of 274 galaxies around 9885 km s^{-1} corresponds to the cluster members

2.7 Figure 2.31 shows the iso-recession velocity curves of the galaxy NGC 5033 deduced from the Doppler shift of the 21 cm line of atomic hydrogen. The curves are superimposed on an optical image of the galaxy.

(a) What is the redshift of NGC 5033. By neglecting its peculiar velocity, estimate its distance as a function of h_{70}.
(b) The visible angular radius of NGC 5033 is about 3 arcmin. What is the visible radius as a function of h_{70}?
(c) What is the rotation velocity far from the galactic center? Take into account the galaxy inclination by supposing that the galaxy would appear to be circular if viewed face-on.
(d) Estimate the mass of NGC 5033 that is within 6 arcmin of the galactic center (in units of $M_\odot$ and as a function of h_{70}).
(e) NGC 5033 has an apparent magnitude in the V band of 10.1. What is its absolute magnitude and its luminosity (in units of $L_{\odot V}$) as a function of h_{70}? What is its mass-to-light ratio?

2.8 The most reliable distance indicators out to $\sim$ 50 Mpc are Cepheid variable stars. The most reliable method of calibrating the luminosity-period relation of Cepheids is to use the large number of Cepheids observed in the Large Magellanic Cloud (LMC). This method of calibration obviously requires a knowledge of the LMC distance.

One of the most direct measurements of the LMC distance uses "eclipsing binaries." Such systems consist of two orbiting stars whose orbital plane is oriented such

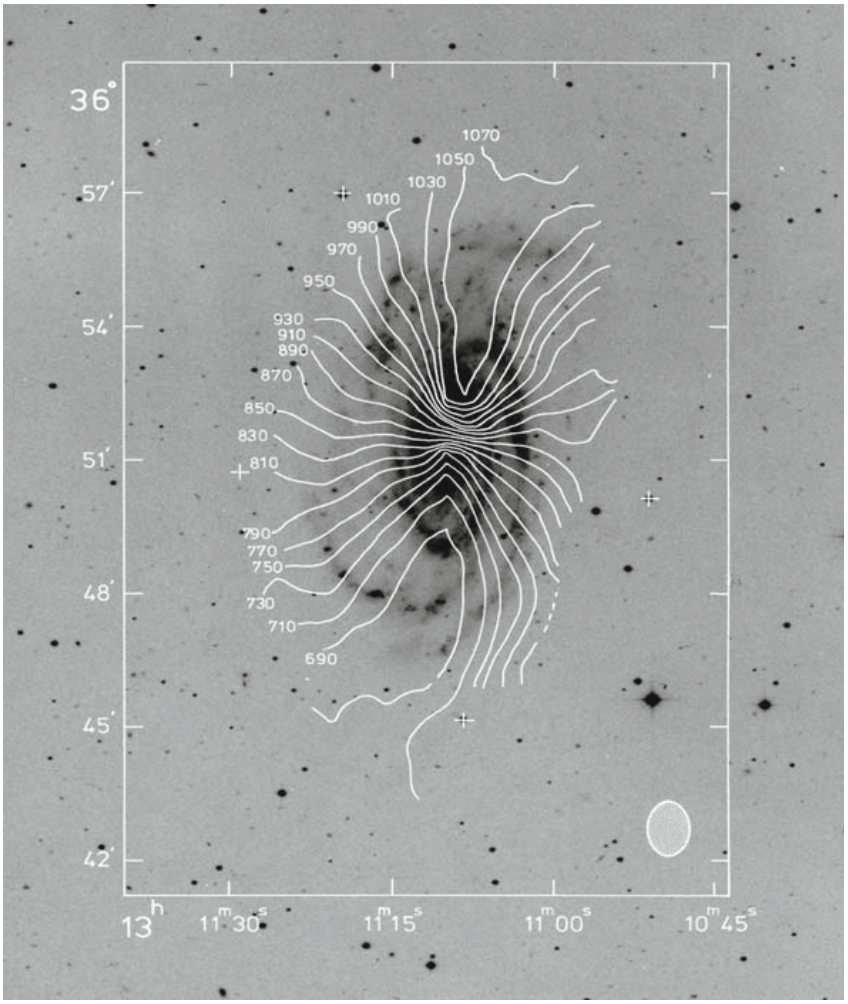

Fig. 2.31 The iso-recession-velocity curves of the galaxy NGC 5033 deduced from the Doppler shift of the 21 cm line of atomic hydrogen [102]. The curves are superimposed on an optical image of the galaxy. The angular scale of the greater dimension is in arcmin. Courtesy of A. Bosma

that, viewed from Earth, the two stars periodically eclipse each other. For eclipsing binaries at the distance of the LMC, the two stars generally have an angular separation that is so small that the two stars cannot be optically resolved. Rather, they appear as a single star with a periodic luminosity due to the periodic eclipses.

Figure 2.32 shows the "light curve" (apparent magnitude versus time) of the binary system HV2274 in the LMC [103]. Two eclipses are present with a period of 5.726 days. The magnitude change of 0.75 during the eclipses corresponds to a factor of two in flux indicating a total eclipse of two stars of equal luminosities and radii.

The spectral lines of the two stars do not coincide because of the Doppler shift due to their orbital motion. It is therefore possible to determine independently the

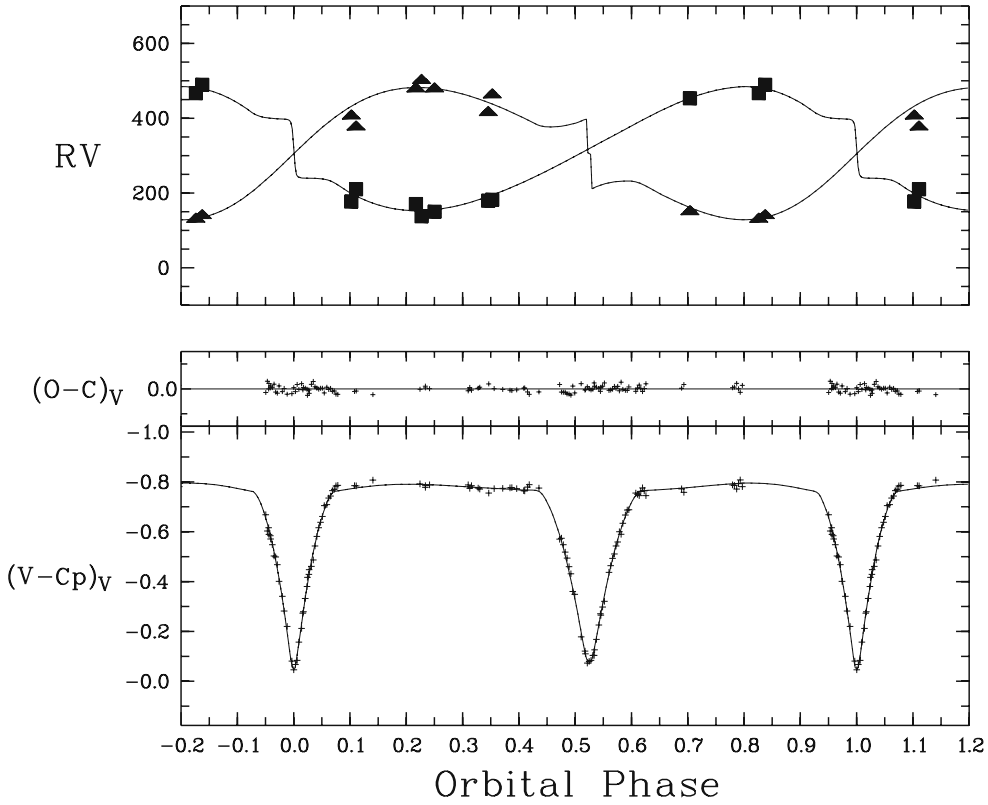

Fig. 2.32 The binary system HV2274 in the LMC [103]. The *upper panel* shows the recession velocity of the two stellar components as a function of the orbital phase (period = 5.726 days). The *lower panel* shows the light curve (apparent magnitude versus time)

recession velocities of the two stars. The two velocities as a function of time are also shown in Fig. 2.32.

(a) Estimate the orbital velocity of the two stars and the radius of the (circular) orbit.
(b) Supposing that the two stars have equal masses, estimate their mass (in units of $M_\odot$).
(c) Use the durations of the eclipses to estimate the common radius of the two stars (in units of $R_\odot$).
(d) The surface temperature of the two stars is $\sim$ 23 000 K. The measured flux indicates, via (2.1), an angular size of $D/R = 9.48 \times 10^{-12}$. Estimate the distance R to HV2274. After a small correction for the relative distance between HV2274 and the center of the LMC, the authors of [103] give an LMC distance of 45.77 ± 1.6 kpc.
(e) Figure 2.5 shows the apparent magnitudes of LMC Cepheids as a function of their periods. Using the distance to the LMC, transform the apparent magnitudes into absolute magnitudes. Compare these magnitudes with those of Cepheids with distances determined by parallax [44], $M_V = -2.81 \log P - 1.43 \pm 0.16$

(period P in days). Compare the value of H_0 that would be estimated using Hipparcos Cepheids with that using LMC Cepheids.

2.9 It is perhaps surprising that the luminosity of a star can be estimated theoretically without knowing the nuclear reactions that power the star. To see how this can be done, we consider a sphere of radius R containing $N_{\rm p}$ protons and $N_{\rm p}$ electrons in the form of an ideal ionized gas.

(a) if the sphere has a uniform density and is in hydrostatic equilibrium with a mean pressure P and volume V, show that

$$3PV = -E_{\rm g} \sim (3/5)\frac{Gm_p^2 N_{\rm p}^2}{R} \ , \tag{2.35}$$

where $E_{\rm g}$ is the total gravitational energy of the sphere and m_p is the proton mass.
The numerical factor (3/5) in (2.35) applies only to a sphere of uniform density. This is not the case for a star but a nonuniform distribution would simply give a different numerical factor. For the rest of this exercise we will ignore all numerical factors.
Applying the ideal gas law to (2.35), we can estimate the mean temperature T in the star:

$$T \sim \frac{Gm_p^2 N_{\rm p}}{R} \ . \tag{2.36}$$

(b) Supposing that the sphere contains photons in thermal equilibrium at the temperature T, show that the total number of photons inside the star is

$$N\gamma \sim N_{\rm p}^3 \left(\frac{m_p}{m_{\rm pl}}\right)^6 \ , \tag{2.37}$$

where $m_{\rm pl} = \sqrt{\hbar c/G} = 1.2 \times 10^{19}$GeV is the Planck mass. Compare $N\gamma$ with $N_{\rm p}$ for the sun ($N_{\rm p} \sim 10^{57}$).
The photons diffuse in the star before escaping at the surface. The number of collisions in this random walk is of order

$$N_{\rm col} \sim \left(\frac{R}{\lambda}\right)^2 \ , \tag{2.38}$$

where λ is the mean free path of a photon in the star.

(c) Show that the mean escape time for a photon is

$$\tau \sim \frac{N_{\rm p}\sigma}{Rc} \ , \tag{2.39}$$

where σ is the mean photon-particle cross-section in the star. From this, argue that the stellar luminosity is

$$L \sim N_{\rm p}^3 \left(\frac{m_{\rm p}}{m_{\rm pl}}\right)^8 \frac{\hbar c^2}{\sigma} \,. \tag{2.40}$$

For a star like the Sun, the atoms are nearly all ionized except near the surface. It follows that $\sigma \sim \sigma_{\rm T}$ (the Thomson cross-section). For $N = 10^{57}$, compare the luminosity from (2.40) with $L_\odot$.

A more careful management of the numerical factors multiplies the above result by $\pi^4/(5 \times 3^8) \sim 3 \times 10^{-3}$ [104]. This gives an agreement with the observed solar luminosity that is reasonable considering the approximations involved in the calculation.

We note that (2.40) predicts that a stellar luminosity is proportional to the third power of its mass, in good agreement with observations.

If the luminosity of a star depends only on its mass, one can ask what is the role of the nuclear reactions that power the star. The answer is that they allow the star to burn *longer* at a stable radius. A star begins its life as a diffuse cloud that is too cold to initiate nuclear reactions. It nevertheless radiates photons as required by (2.40). In so doing, it radiates energy and total energy conservation requires the star's radius to diminish. As the star becomes smaller, its temperature rises until nuclear reactions are ignited. At this point, a stable regime is reached where the energy radiated is replaced by the energy liberated by the nuclear reactions.

2.10 Roughly 10% of the mass of large galactic clusters is contained in ionized intergalactic gas in hydrostatic equilibrium. This gas produces photons via bremsstrahlung:

$$\mathrm{e}^- \mathrm{p} \rightarrow \mathrm{e}^- \mathrm{p} \gamma \,. \tag{2.41}$$

Theoretical and observed spectra are shown in Figs. 2.33 and 2.34.

Unlike the photons produced in stars, these photons escape directly from the cluster:

(a) The largest clusters contain $\sim 10^{14} M_\odot$ of ionized hydrogen in a radius of ~ 1 Mpc. Verify that the mean free path of photons due to Thomson scattering in the cluster is greater than the cluster radius.

(b) The large angle Rutherford scattering cross-section is $\sim \sigma_{\rm T}/(v/c)^4$. Verify that the effective mean free path of electrons (scattering on protons) in the cluster is less than the cluster radius. This justifies the assumption that the electrons and protons form a thermal gas in hydrostatic equilibrium.

For non-relativistic electrons, the differential cross-section for bremsstrahlung production of photons of energy $E\gamma$ is approximately [106]

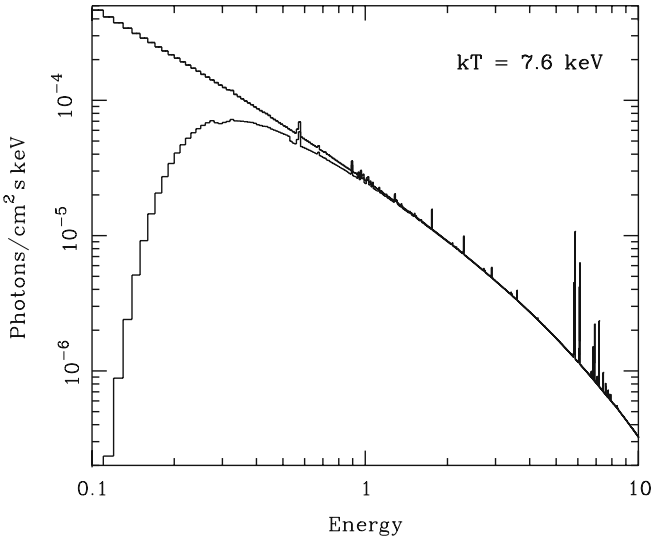

Fig. 2.33 The theoretical X-ray spectrum from a galactic cluster of temperature 7 keV. The spectrum follow the $1/E$ bremsstrahlung cross-section at low energy and then is exponentially cutoff at energies above the temperature. Recombination lines for iron are seen around 6 keV. The second *curve* that has a suppressed flux at low energy shows the effect of absorption in the Milky Way. Courtesy of Monique Arnaud

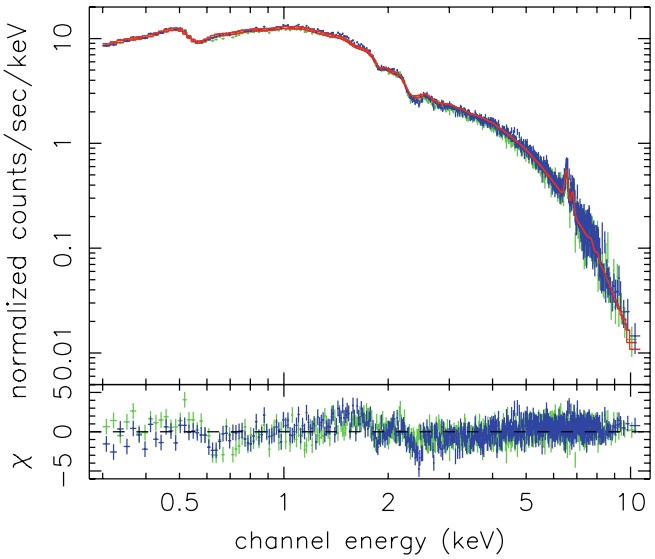

Fig. 2.34 The observed X-ray spectrum from the Coma galaxy cluster as observed by the XMM satellite [105]. The structures in the spectrum around 2 keV and 0.5 keV are due to the varying efficiency of the detection system. The fitted cluster temperature is $kT = 8.25$ keV. Courtesy of Monique Arnaud

$$\frac{\mathrm{d}\sigma}{\mathrm{d}E_\gamma} \sim \alpha \, \frac{c^2}{v^2} \, \frac{\sigma_\mathrm{T}}{E_\gamma} E_\gamma \ll (1/2) m_e v^2 \ , \tag{2.42}$$

where $\alpha \sim 1/137$ is the fine-structure constant, $v \ll c$ is the electron–proton relative velocity, and σ_T is the Thomson cross-section.

Using a line of reasoning that will be justified in Chap. 6, we know that the production rate per unit volume of photons is proportional to the differential cross-section (2.42), to the electron density n_e, to the proton density $n_\mathrm{p} \sim n_\mathrm{e}$, and to the mean electron–proton velocity:

$$\frac{\mathrm{d}N_\gamma}{\mathrm{d}t\mathrm{d}V} \sim n_\mathrm{p}^2 \, v \frac{\mathrm{d}\sigma}{\mathrm{d}E_\gamma} \sim \frac{c}{v} \, n_\mathrm{p}^2 \alpha c \frac{\sigma_\mathrm{T}}{E_\gamma} \ . \tag{2.43}$$

(c) Integrate this expression up to a photon energy cutoff given by the temperature of the cluster T to find the total X-ray luminosity (energy/time):

$$L_x \sim n_\mathrm{p}^2 \alpha c \sigma_\mathrm{T} \sqrt{m_\mathrm{e} c^2 T} D^3 \ , \tag{2.44}$$

where D is the diameter of the cluster.

(d) Show that the total number of baryons, N_b, in the cluster can be estimated from the observed X-ray flux, f_x:

$$N_\mathrm{b}^2 \sim \frac{f_\mathrm{x} R^5 \theta^3}{\alpha c \sigma_\mathrm{T} \sqrt{m_\mathrm{e} c^2 T}} \ , \tag{2.45}$$

where θ is the observed angular diameter of the cluster and R is the distance to the cluster. This formula shows that if a cluster redshift is used to estimate the cluster's distance, the measured total baryonic mass in the cluster scales as $h_{70}^{-5/2}$.

(e) Modify (2.35) so that the thermal pressure supports only the baryonic mass of the cluster and thereby show that the total cluster mass in terms of the X-ray temperature is

$$M_\mathrm{tot} \sim \frac{6kTR}{Gm_\mathrm{p}} \tag{2.46}$$